

Radiation hardness investigations of Al_2O_3 for MeV/u ions at GSI

ARIES-ADA Workshop on Scintillation Screens

Krakow, 2nd of April 2019

Presented Peter Forck, GSI

Work performed by Stefan Lederer (PhD student 2012 to 2016)

with support by Eiko Gütlich, Beata Walasek-Höhne, GSI

Wolfgang Ensinger, TU-Darmstadt

S. Akhmadaliev, J. von Borany, HZDR, Dresden, et al.

Al_2O_3 ceramics properties:

- Ionic crystallites
- Ceramic sintered from grains; here mainly with average grain size $\langle d \rangle \approx 5 \mu\text{m}$
- Intrinsic scintillator: Light emission originated from vacancies in lattice
↔ scintillation caused by imperfections (boundaries & inside crystal)

Outline of the talk: Experimental findings, interpretations and conclusions

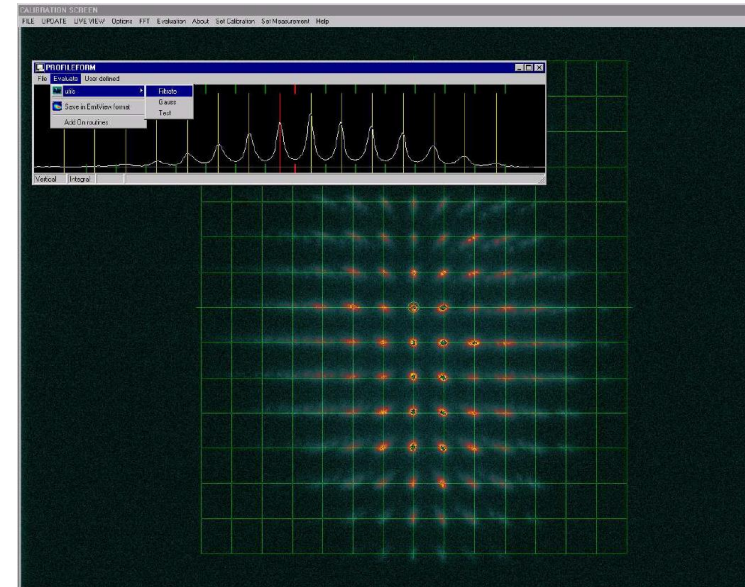
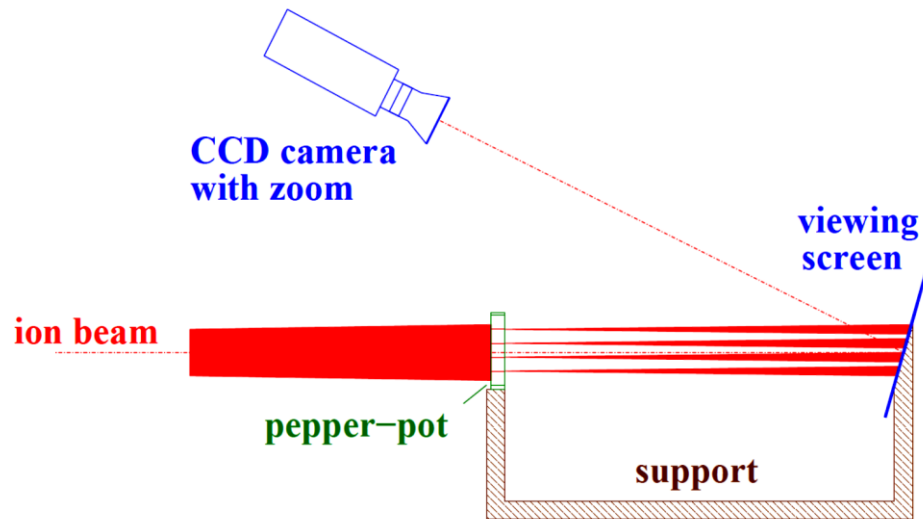
Motivation: Pepper-pot Emittance Measurement

GSI ion LINAC: All ions $E_{kin} = 1.4 \dots 11.4 \text{ MeV/u} \Rightarrow$ typ. range $R = 10 \dots 100 \mu\text{m}$, max. P_{pulse} up to 100kW

Goal for pulsed high current LINAC: Measurement within one pulse of typ. $t_{pulse} \approx 100 \mu\text{s}$

- High particle density at spots
 - If horizontal and vertical direction coupled \rightarrow 2-dim evaluation **required** e.g. for ECR source
- \Rightarrow **Requirements:** Correct reproduction \rightarrow linearity, temperature insensitivity, radiation hardness

Example: Ar^{1+} ions at 1.4 MeV/u on Al_2O_3 , screen image from single shot at GSI



Results in 2000 – 2003:

Pepper-pot differs from slit-grid emittance measurement

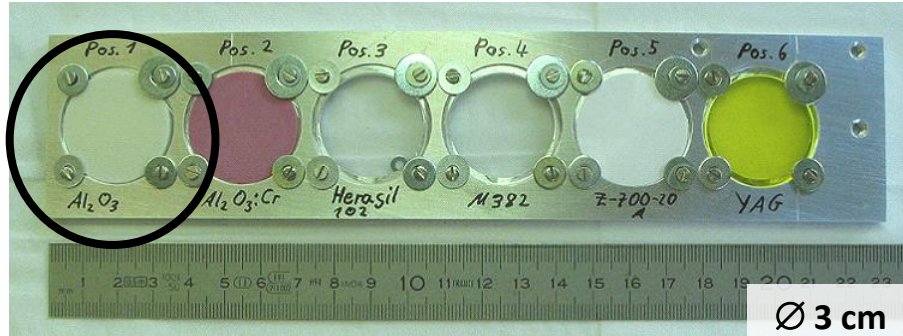
Possible reason: Image properties of scintillator

- \Rightarrow Investigation started year 2007 with interesting results....
- \Rightarrow This talk: properties of Al_2O_3 as simple **intrinsic** scintillator

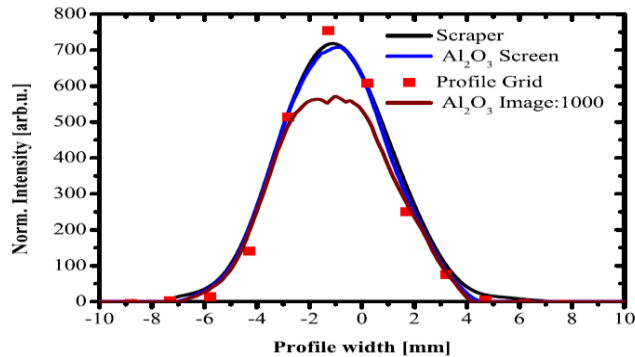
Scintillation Screen Investigations with different Scintillators

Due to high current, ceramics or glass is preferred \Rightarrow test of entire profile

Target ladder for irradiation:

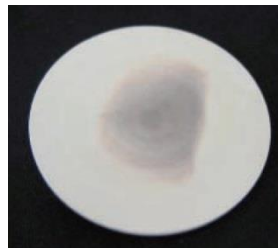


Decrease of luminescence at maximum \Rightarrow image width increase **wrongly**:

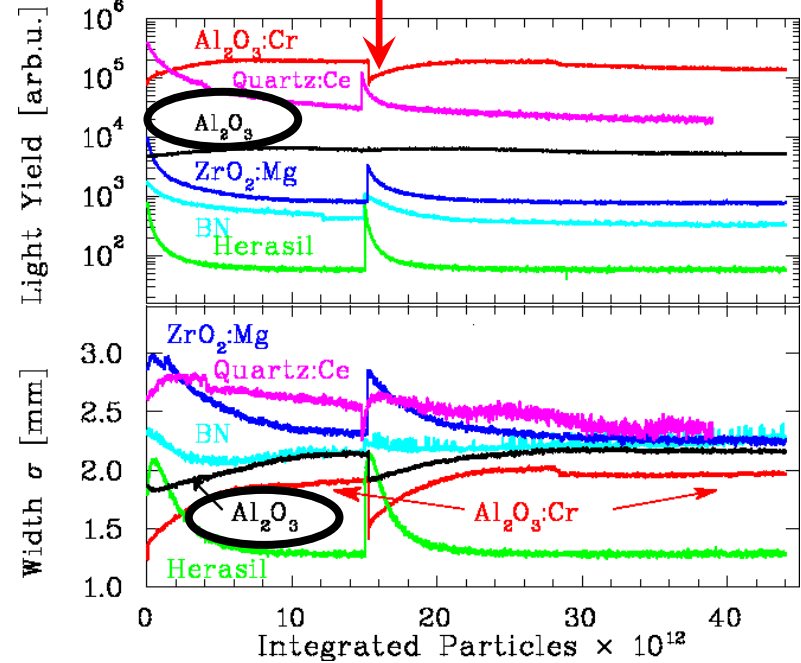


Reasons:

- Thermal quenching
- Material lattice modification i.e. color center by radiation



After 750 pulses: 3 min break to reach ambient temperature



High current beam parameter:

Ar^{10+} at 11.4 MeV/u, 2200 pulses, $\approx 2 \times 10^{10}$ ppp
 $I_{pulse} = 300 \mu A$, $P_{pulse} = 14 kW$, $t_{pulse} = 100 \mu s$, 2.6 Hz

Target: Range $R = 84 \mu m$ for Al_2O_3 ($\rho = 4 g/cm^3$)

Recording: Entire optical spectrum

E. Gütlich (GSI) et al., BIW 2008

Thermal Quenching for Al_2O_3

Thermal quenching:

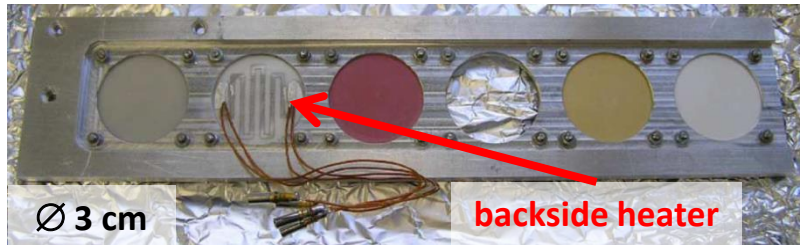
Non-radiative transition to other electronic configuration

⇒ no optical photon emission

⇒ enhancement for higher temperature

Experimental realization:

Heating of scintillator during irradiation in addition to beam



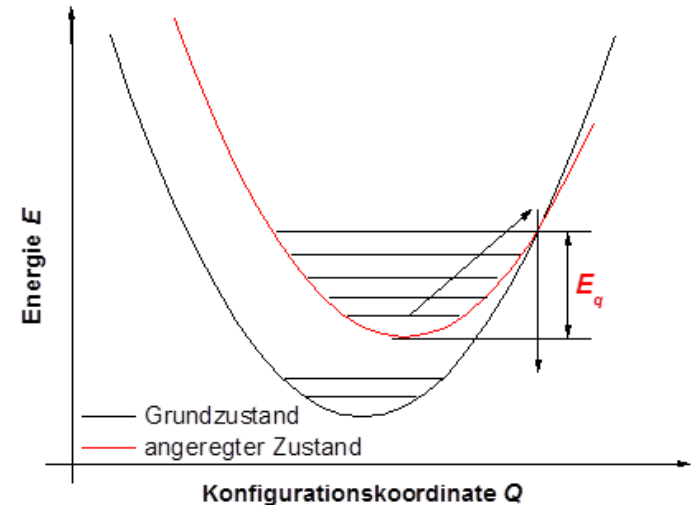
Results (entire optical spectrum):

Room temperature:

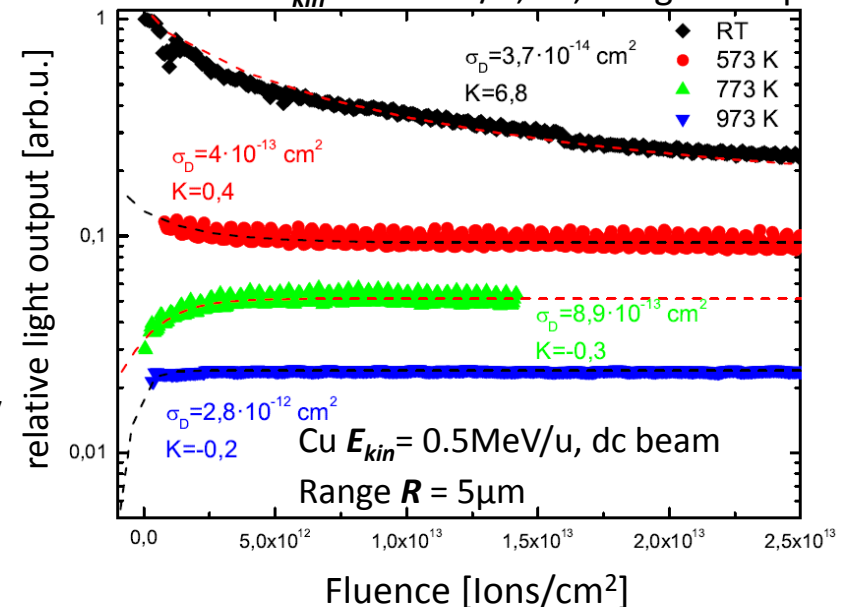
- Decrease of light output due increasing temperature

External heating:

- Lower light output due to quenching
 - Stable due to less relative temperature change
 - Could be understand in terms of color center mobility
- ⇒ Practical application: 'in situ' tempering for annealing



Beam: Cu $E_{kin} = 0.5\text{MeV/u}$, dc, Range $R = 5\mu\text{m}$



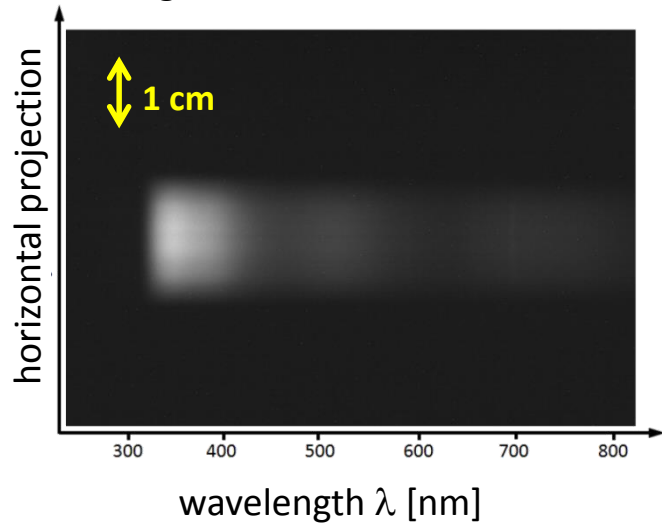
S. Lederer (GSI) et al., NIM B 359, 2015

Setup for Spectroscopic Investigations

Detailed investigations at TANDEM @ HZDR in Dresden:
 Cu ions $E_{kin} = 0.5 \text{ MeV/u}$, $R = 5 \text{ }\mu\text{m}$, $I_{beam} = 0.01 \dots 100 \text{ nA dc}$
 for spectrum and image width, variation of temperature

Image spectrometer: Horiba CP 140

Over all wavelength interval: $\lambda = 320 \dots 700 \text{ nm}$

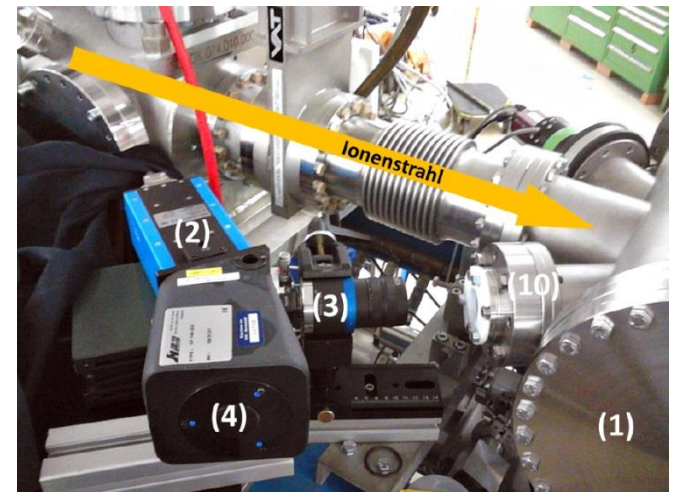
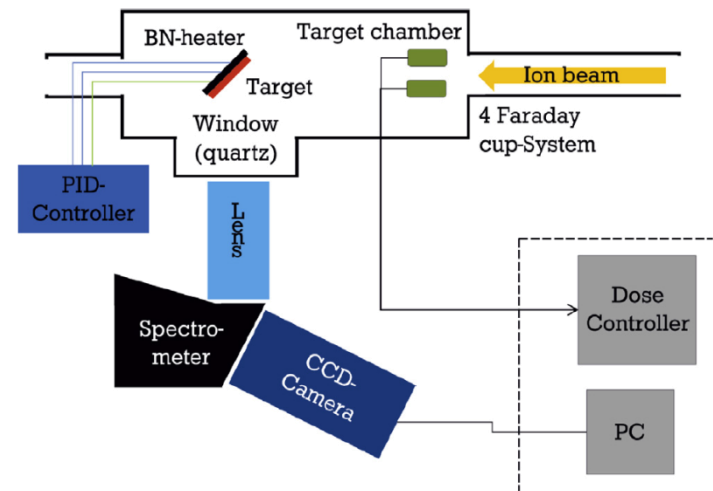


Procedure:

- Irradiation of individual samples on target wheel
- Online observation during irradiation
- Offline investigations of individual samples

Detailed results in

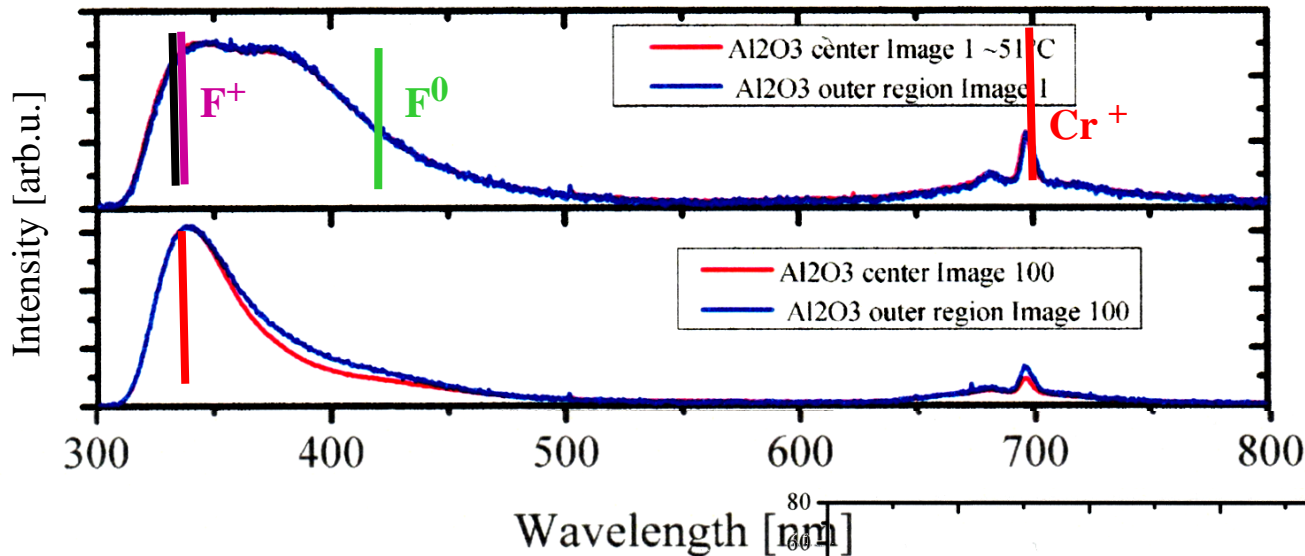
- S. Lederer et al., NIM B 359 (2015) & NIM B 365 (2015)
- PhD thesis, TU-Darmstadt tuprints.ulb.tu-darmstadt.de/5282/



(3) lens, (4) spatial resolving spectrometer,
 (4) CCD camera

Spectroscopic Results for Profile Reading of Al₂O₃

Example for investigations: Wavelength spectra and image reproduction for Al₂O₃



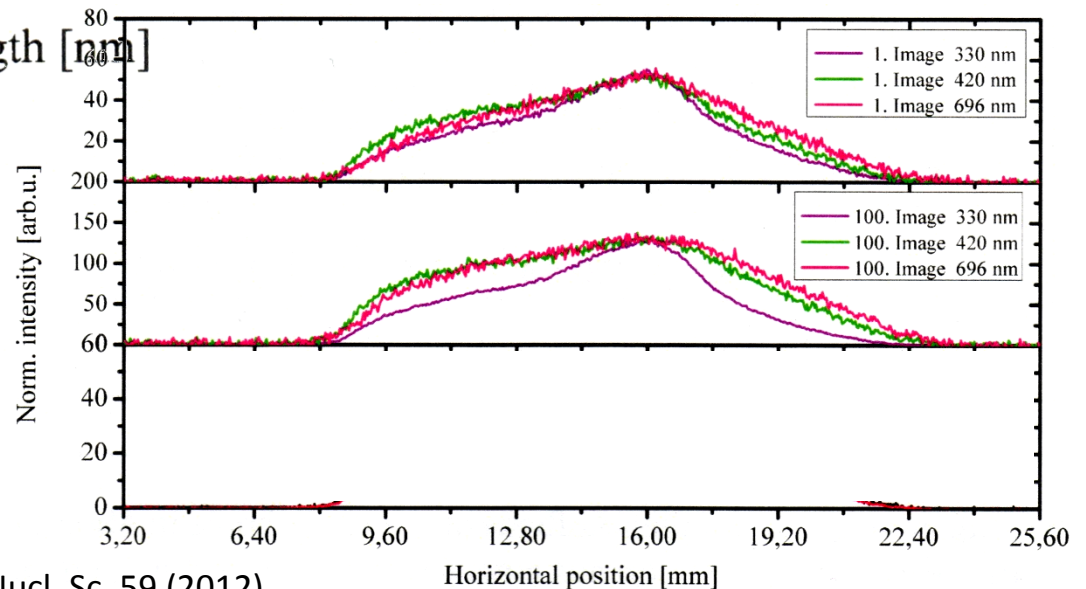
Beam parameter @ GSI:
 Ca¹⁰⁺, 4.8 MeV/u $I = 30 \mu\text{A}$,
 duration $t_{pulse} = 3.3 \text{ ms}$, 1Hz
 5×10^{10} ppp, $P_{pulse} = 0.6 \text{ kW}$

Spectrum influenced by:

- Temperature → thermal quenching
- Material modification by radiation

But:

Some transitions are less sensitive
 Al₂O₃: color center F⁺ with $\tau = 2 \text{ ns}$
 Goal: Understanding the physics

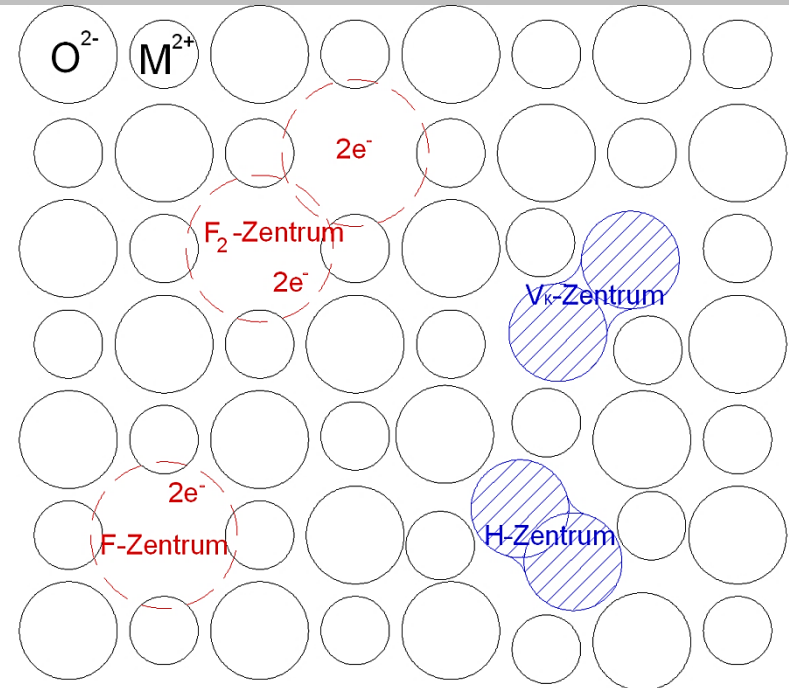


E. Gütlich (GSI) et al., DIPAC'11, SCINT'11: IEEE Nucl. Sc. 59 (2012)

Color Centers for Al₂O₃ as intrinsic Scintillator

Primary radiation defects:

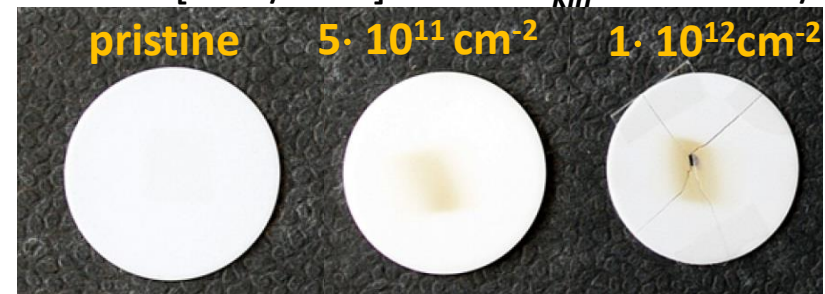
- **Low dose** ($D < 100$ kGy):
Displacement and Frenkel pairs
 - **High dose:**
Increasing probability for clusters
Compensation of charges by
electron & hole capture → luminescence
- ⇒ **Color center** ('**F-center**') at O²⁻ vacancy
 ⇒ **H/V_k** center at Al³⁺ vacancy



Properties for Al₂O₃:

Color Center	# O ²⁻ vacancies	# trapped electrons	Emission λ [nm]
F	1	2	413
F⁺	1	1	326
F ₂	2	4	322
F ₂ ⁺	2	3	380

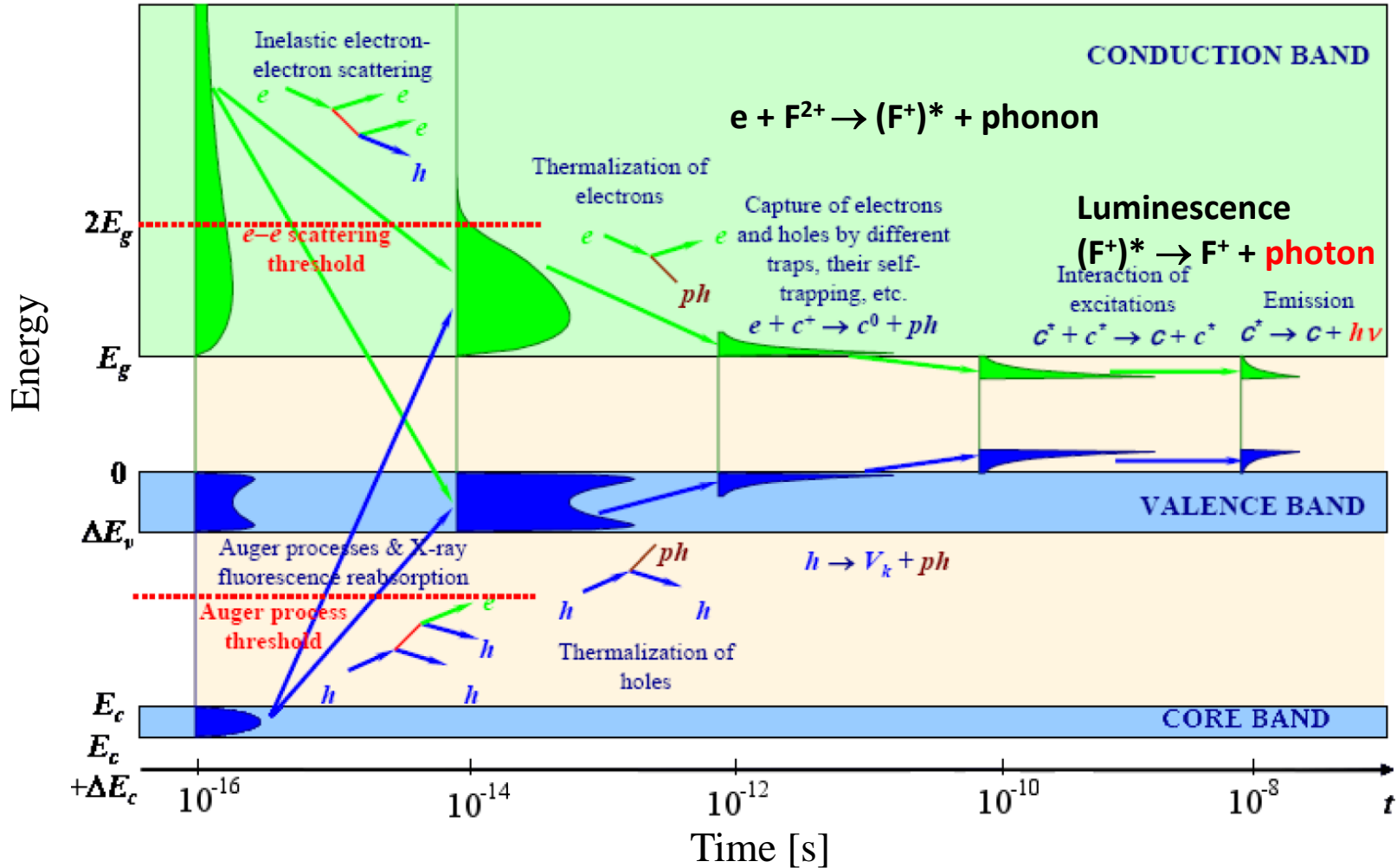
Macroscopic result: Coloring of material
 Fluence [Ions/cm²] for Au $E_{kin} = 5.9$ MeV/u



Simplified Scheme of an intrinsic Scintillator

General mechanism for an intrinsic scintillator with activators

i.e. color centers, self-trapped excitons or holes with partly large extension for wave-function

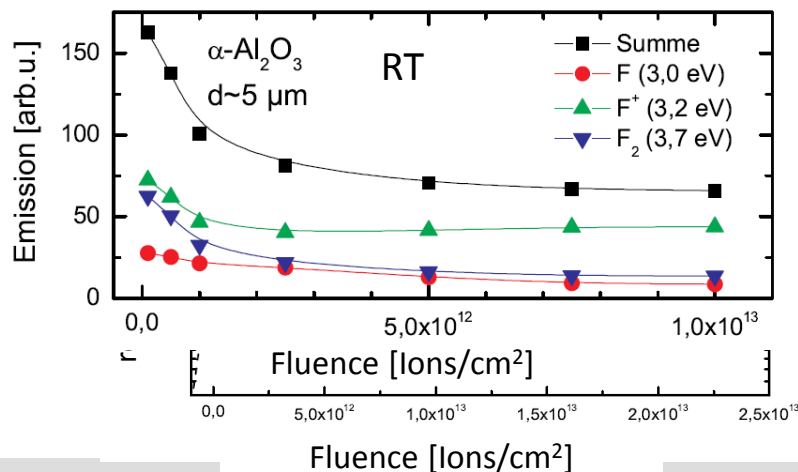


P. Lecoq et al.: Inorganic scintillators for Detector systems, Springer Verlag 2006

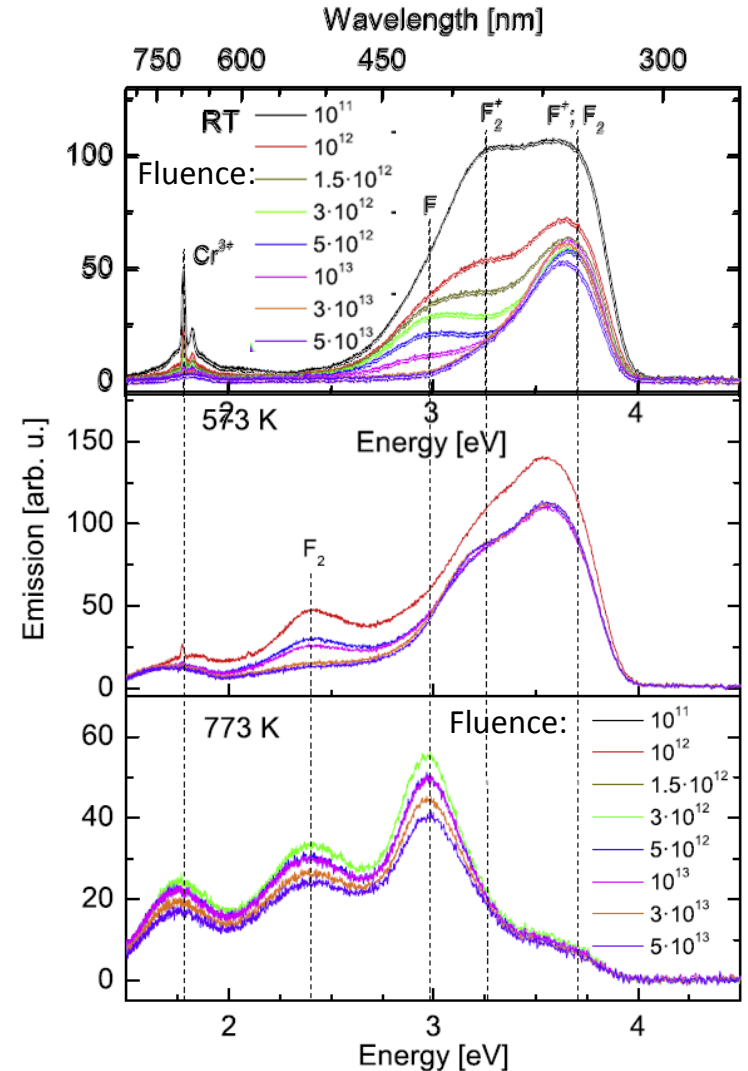
Temperature & spectral dependent Emission for Al_2O_3

Light emission for heated Al_2O_3 for dc beams i.e. in equilibrium:

- **Pristine:** Color centers & Cr^{3+} (at 700 nm)
 - **Room temperature & increasing fluence:**
 1. Suppression of Cr^{3+} & some color center
 2. Less reduction of color center F^+ @ 326 nm
 - **Heating to 300 °C & increasing fluence:**
 1. Thermal quenching of most transitions
 2. F^+ @ 326 nm strongest line
 - **Heating to 500 °C & increasing fluence:**
 1. 'In-situ' color center mobility, stable light output
 2. F^+ @ 326 nm less emission, stable emission
- ⇒ Optimal temperature ≈ 400 °C for F^+



Beam: Cu $E_{kin} = 0.5\text{MeV/u}$, dc beam Range $R = 5\mu\text{m}$



Cut by spectrometer at 300 nm
S. Lederer (GSI) et al., NIM B 359, 2015

Birks Model as empirical Description for Radiation Effects

Empirical Birks model for radiation damage:

- Light yield $S(\Phi)$ as function of fluence Φ can be described by

$$S(\Phi) = S(0) \cdot \frac{1}{1 + K \cdot [1 - \exp(-\sigma_D \Phi)]}$$

$K = \frac{k_q}{k_f + k_i}$: effect on emission as ratio between:

k_q : quenching by damage i.e. displacement

k_i : internal quenching

k_f : regular luminescence emission

Depictive description:

1. Radiation leads to displacements
⇒ lower luminescence due to quenching
2. Partly destroyed material
3. Finally saturation of 'destroyed material' :
probability for 'landing' in a vacancy increases

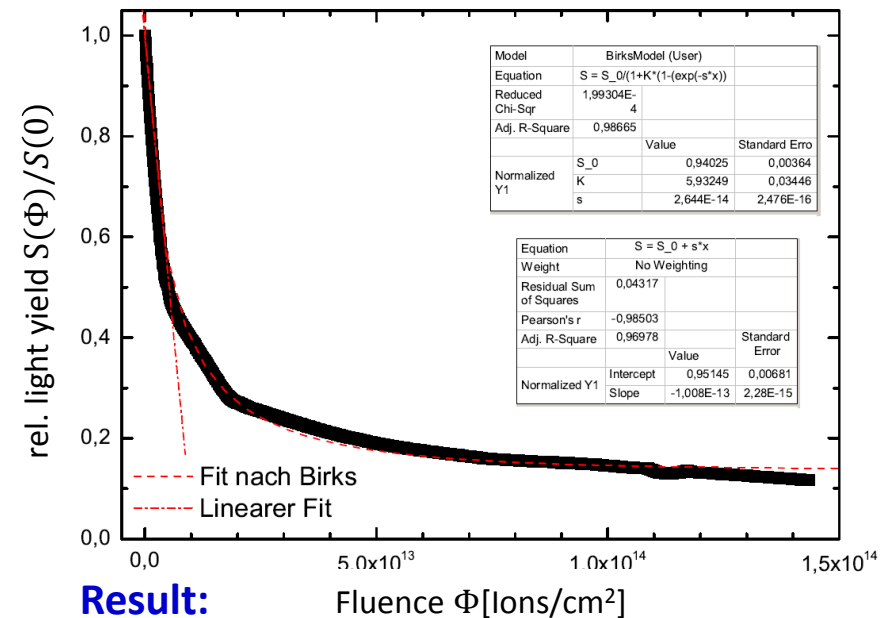
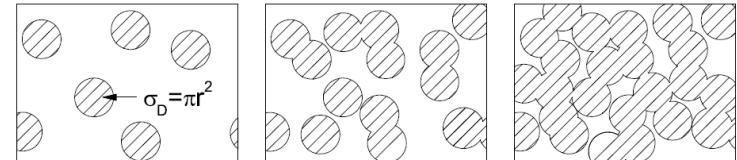
⇒ **Nearly no net effect for large damage**

⇔ **'stable' scintillation (on lower level)** ⇔ **'damage stops'**

Beam: Cu $E_{kin} = 0.5\text{MeV/u}$, dc beam, Range $R = 5\mu\text{m}$

Material property for Al_2O_3 :

linear regime sub-linear regime saturation



Result: Fluence Φ [Ions/cm²]

Initial: Large initial radiation damage

Final: Lower, but nearly constant light yield

Birks Model for other intrinsic Scintillators

Empirical Birks model for radiation damage:

- Light yield $S(\Phi)$ as function of fluence Φ can be described by

$$S(\Phi) = S(0) \cdot \frac{1}{1 + K \cdot [1 - \exp(-\sigma_D \Phi)]}$$

$K = \frac{k_q}{k_f + k_i}$: effect on emission as ratio between:

k_q : quenching by damage i.e. displacement

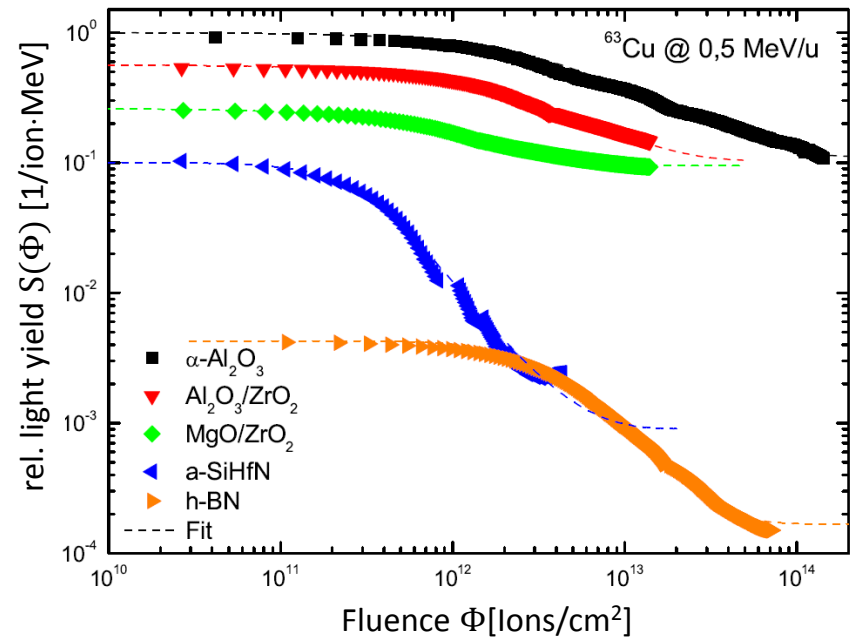
k_i : internal quenching

k_f : regular luminescence emission

Results:

- General behavior for intrinsic scintillators
- Properties depend significantly on lattice structure
- Al_2O_3 **ceramics** is more radiation hard than others
- Depend strongly on crystallite structure & amount of initial vacancies
i.e. average grain size $\langle d \rangle$ and production method

Beam: Cu $E_{kin} = 0.5\text{MeV/u}$, dc beam Range $R = 5\mu\text{m}$



Material	$\sigma_D [10^{-14} \text{ cm}^2]$	K
$\alpha\text{-Al}_2\text{O}_3 \langle d \rangle = 5\mu\text{m}$	2,6	5,9
$\text{Al}_2\text{O}_3/\text{ZrO}_2$	8,2	4,3
MgO/ZrO_2	38,6	1,8
a-SiHfN	46,1	110,0
BN	9,4	23

S. Lederer (GSI) et al., NIM B 359, 2015

Radiation Damage of Al_2O_3 as a Function of Energy Loss

Radiation damage depends on initial energy loss
i.e. amount of displacements per ion.

Results at LINAC energies:

- Energy loss $S_e \equiv dE/dx \propto Z^2$ for ion of charge Z
- Initial light yield: light ion / heavy ion $\approx 20\%$
- Significant difference of radiation damage per ion

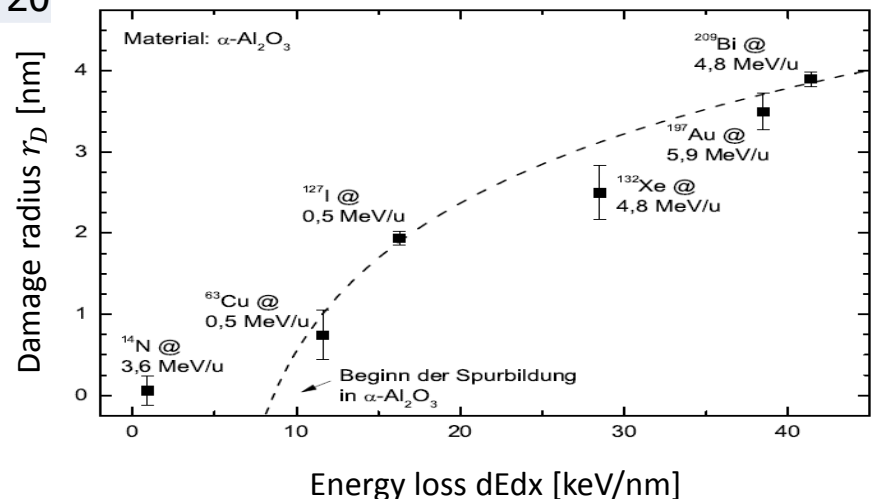
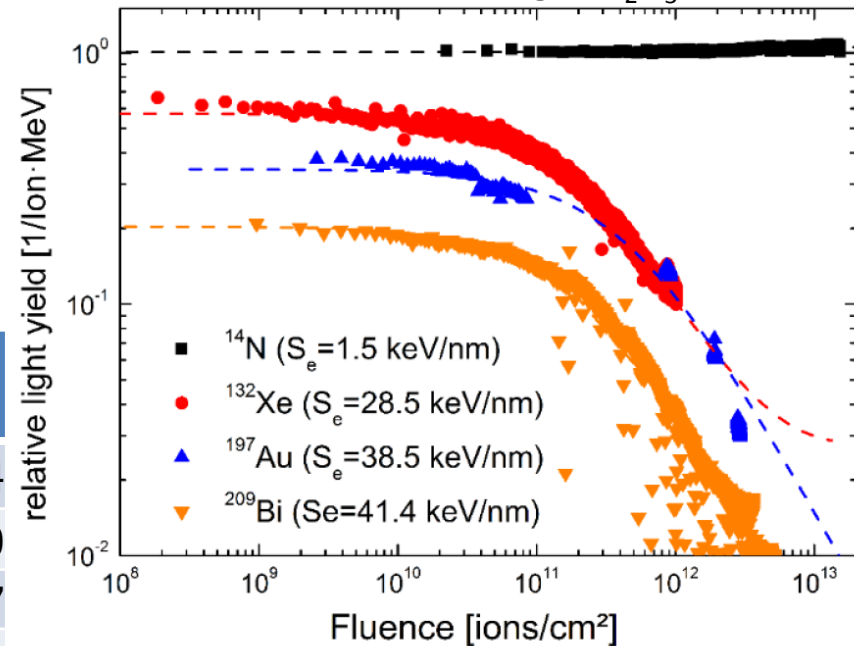
Ion	Energy [MeV/u]	Range R [μm]	dE/dx [keV/nm]	Damage σ_d [10^{-14}cm^2]	Quench K
^{14}N	3,6	26	1,5	0.03	0.04
^{132}Xe	4,8	27	28,5	20	20
^{197}Au	5,9	37	38,5	38	17
^{209}Bi	4,8	31	41,4	48	20

Energy dependent damage:

Damage radius $r_D = \sqrt{\sigma_D/\pi}$ depends on

- Energy loss
- Ion velocity

Beam: Different beam at GSI, target Al_2O_3



Radiation Damage of Al_2O_3 as a Function of Ion's Energy

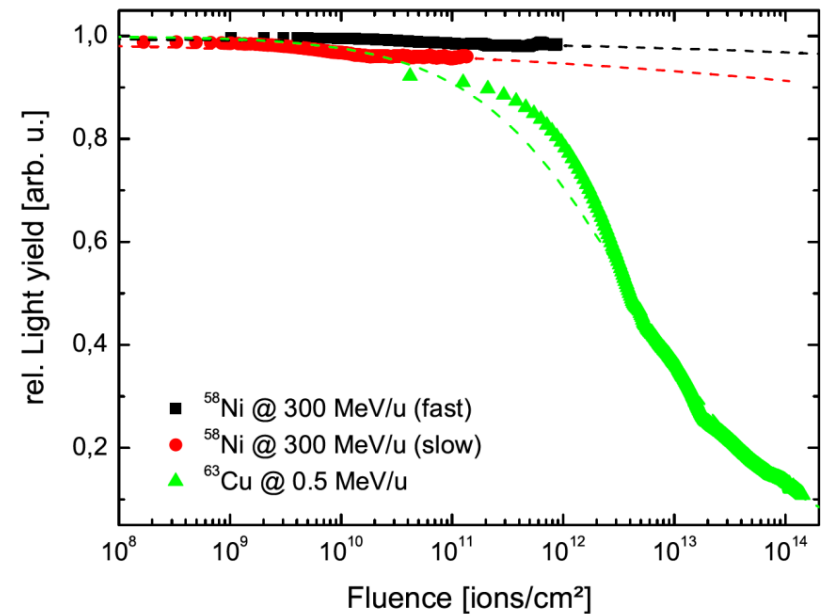
Results for different energies:

Comparison of comparable ions at different energies
(Tandem @ HZDR and behind SIS @GSI)

- Radiation hardness is significantly increased at higher energies
- Energy loss for Cu @ 0.5 MeV/u: $dE/dx = 12 \text{ keV/nm}$
- Energy loss for Ni @ 300 MeV/u: $dE/dx = 0.9 \text{ keV/nm}$

⇒ Radiation damage reduced for 'relativistic' ions

Beam: Cu at HZDR, Ni behind GSI synchrotron



Atomistic Description of Damage: Nuclear Stopping

Mechanisms of projectile ↔ target interaction

1. Simple picture of energy loss

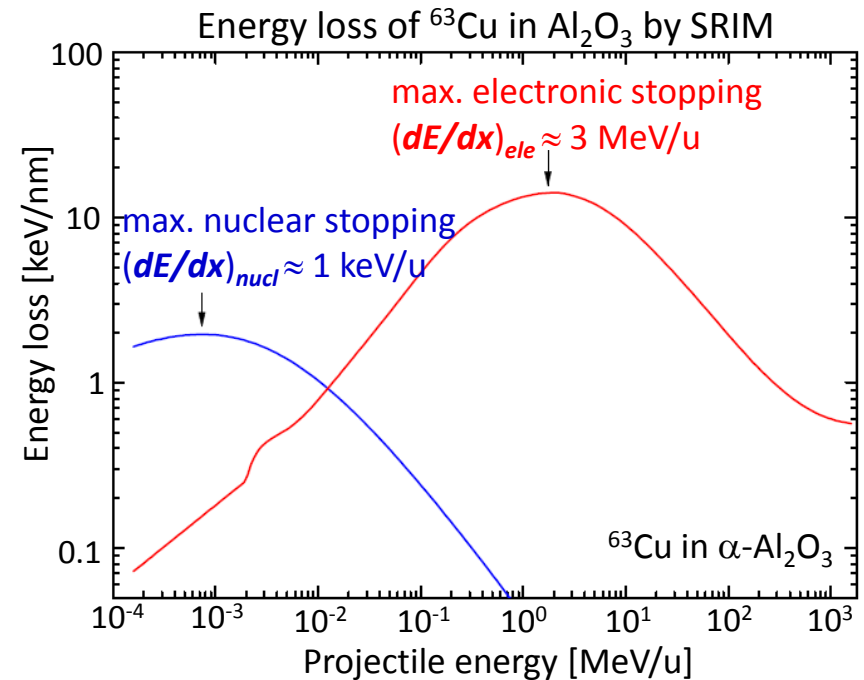
Nuclear stopping: Binary collision of ion with **one** target nucleus

→ too low cross section for damage

2. Thermal spike model

Electronic stopping: Collision of ion with **many** target electrons

⇒ leading to many defects for MeV/u ions

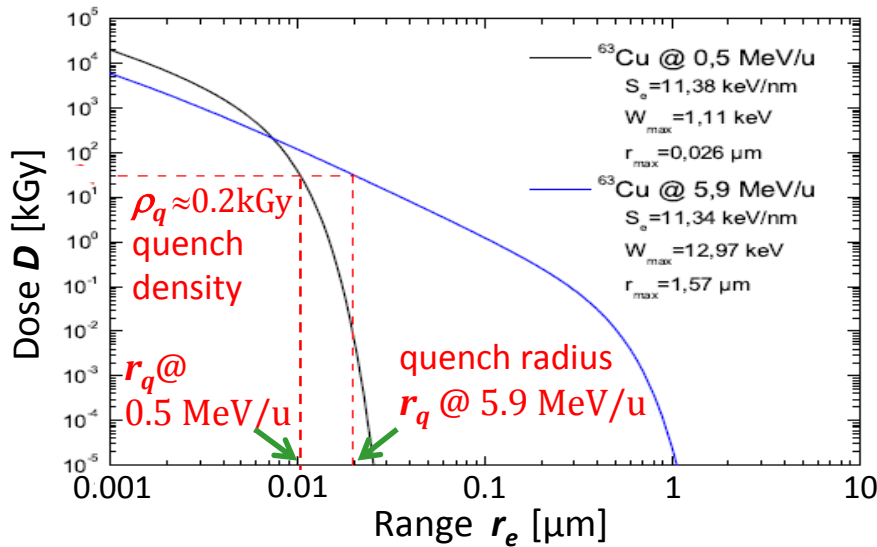


Atomistic Description of Damage: Thermal Spike by electronic Stopping

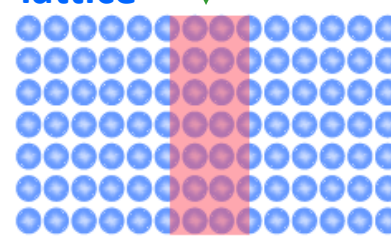
2. Thermal spike model

Electronic stopping: Collision of ion with **many** target electrons

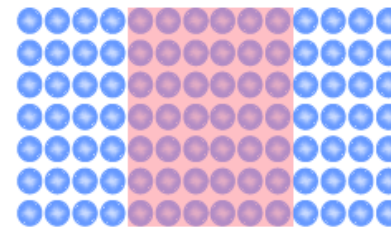
- Max. e⁻ kin. energy $W_{kin} = 2m_e \beta_{ion}^2 \gamma_{ion}^2$
 \Rightarrow range r_{max} depends on ion velocity β_{ion}^2
- Light yield suppressed for dose $D(r_e) > \rho_q \propto \rho_e$
 'Michaelian model', ρ_q critical quench density
- For ion A^{q+} scaling $dE/dx \propto q^2 \propto \rho_e$, e⁻ density significant track formation for $dE/dx \gtrsim 5$ keV/nm



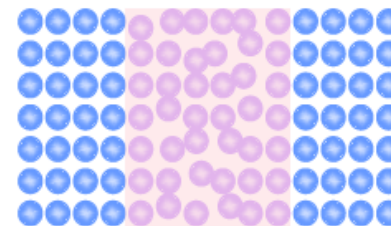
Material modification, 'tracks' for \approx MeV/u ions



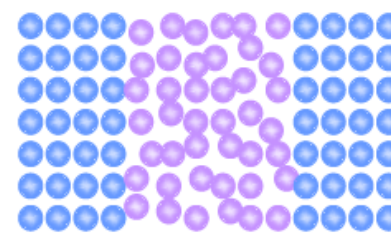
1. Energy deposition by ionization ($\approx 10^{-16}$ s)
 \rightarrow fast δ -electrons



2. Fast thermalization ($\approx 10^{-14}$ s)
 \rightarrow many low energy e⁻



3. Transfer to lattice by e⁻-phonon coupling ($\approx 10^{-12}$ s)
 \rightarrow melting 'thermal spike'



4. Cooling by dissipation ($\approx 10^{-10}$ s)
 \rightarrow defects along ion track
 \Leftrightarrow amorphisation

R. Katz et al., NIM B 107 (1996)

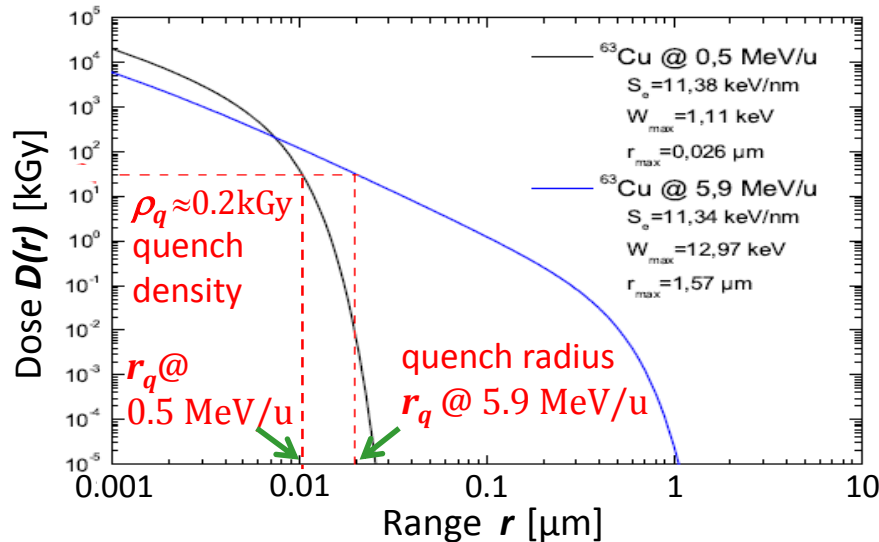
K. Michaelian et al., NIM A 356 (1995) & NIM B 194 (2002)

Atomistic Description of Damage: Thermal Spike by electronic Stopping

2. Thermal spike model

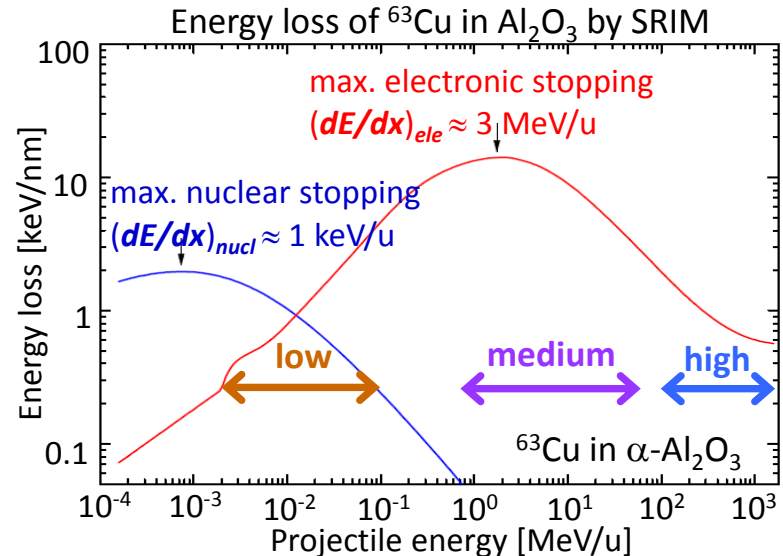
Electronic stopping: Collision of ion with **many** target electrons

- Max. e⁻ kin. energy $W_{kin} = 2m_e \beta_{ion}^2 \gamma_{ion}^2$
 \Rightarrow range r_{max} depends on ion velocity β_{ion}^2
- Light yield suppressed for dose $D(r_e) > \rho_q \propto \rho_e$
 'Michaelian model': ρ_q critical quench density
- For ion A^{q+} scaling $dE/dx \propto q^2 \propto \rho_e$, e⁻ density
 significant track formation for $dE/dx \gtrsim 5$ keV/nm



Radiation hardness & quenching for **this** process:

- Ion A^{q+}, **medium energy** $1 \text{ MeV/u} < E_{kin} < 100 \text{ MeV/u}$
 large $dE/dx \propto q^2_{eff}$, large quench $r_q \Rightarrow$ **large damage**
- Proton, **medium energy** $1 \text{ MeV} < E_{kin} < 100 \text{ MeV}$
 low $dE/dx \Leftrightarrow D(r)$, low quench $r_q \Rightarrow$ **low damage**
- Ion, **low energy** (e.g. ion source) $E_{kin} < 0.1 \text{ MeV/u}$
 nucl. stopping (other process) \Rightarrow **low damage**
- Ion, **high energy** $E_{kin} > 100 \text{ MeV/u}$
 low $dE/dx \Leftrightarrow D(r)$, low quench $r_q \Rightarrow$ **low damage**

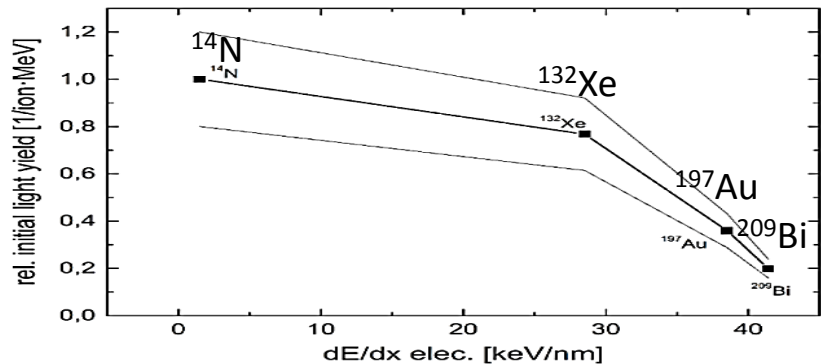


R. Katz et al., NIM B 107 (1996)

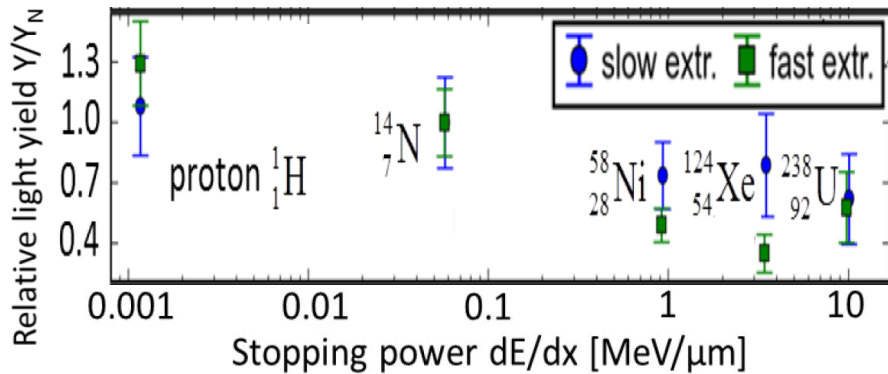
K. Michaelian et al., NIM A 356 (1995) & NIM B 194 (2002)

Comparison of Radiation Damage & Light Yield for different Beams

Light yield for 3.8 ... 5.9 MeV/u ions rel. to N:



Light yield for 300 MeV/u ions relative to N:



Result:

Light yield relative to yield for N

→ stronger decrease for medium energy ions

→ more radiation damage

Explanation:

Related to amorphisation and quenching

Comparison radiation damage: Radiation hardness & quenching for this process:

- Ion Aq^+ , **medium energy** $1 \text{ MeV/u} < E_{kin} < 100 \text{ MeV/u}$
large $dE/dx \propto q^2_{eff}$, large quench $r_q \Rightarrow$ **large damage**
- Proton, **medium energy** $1 \text{ MeV} < E_{kin} < 100 \text{ MeV}$
low $dE/dx \Leftrightarrow D(r)$, low quench $r_q \Rightarrow$ **low damage**
- Ion, **low energy** (e.g. ion source) $E_{kin} < 0.1 \text{ MeV/u}$
nucl. stopping (other process) \Rightarrow **low damage**
- Ion, **high energy** $E_{kin} > 100 \text{ MeV/u}$
low $dE/dx \Leftrightarrow D(r)$, low quench $r_q \Rightarrow$ **low damage**

Ion	Nucl. z	Energy [MeV/u]	dE/dx [keV/nm]	Ratio to N Energy loss dE/dx_{norm}	Ratio to N Light Yield Y_{norm}
^{132}Xe	54	4.8	29	15	58 %
^{209}Bi	83		41	22	20 %
^{132}Xe	54	300	3.5	60	≈ 70 %
^{238}U	92		10	177	62 %

S. Lederer (GSI) PhD thesis, A. Lieberwirth et al., IBIC'16

Color Center Evolution for Al_2O_3 of different Grains

Color center evolution during irradiation:

Test for $\alpha\text{-Al}_2\text{O}_3$ with $\langle d \rangle = 5 \mu\text{m}$:

- Irradiation creates defects
- Migration of color centers possible
- Stabilization for F^+ emission at 3.2 eV = 326 nm

Investigated for $\alpha\text{-Al}_2\text{O}_3$ with $\langle d \rangle = 5 \mu\text{m}$

Sample from BCE special ceramics, Mannheim

Test for sub- μm $\alpha\text{-Al}_2\text{O}_3$ with $\langle d \rangle = 0.5 \mu\text{m}$:

- Much lower **initial** F^+ concentration
⇒ different initial color center conc. & evolution
- For high fluence: Same behavior
i.e. same F^+ concentration

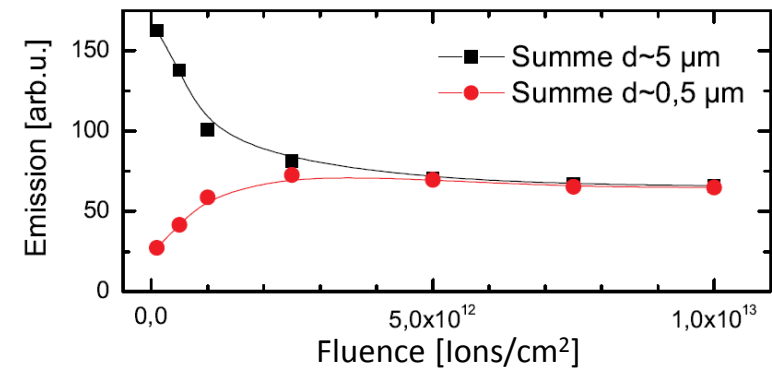
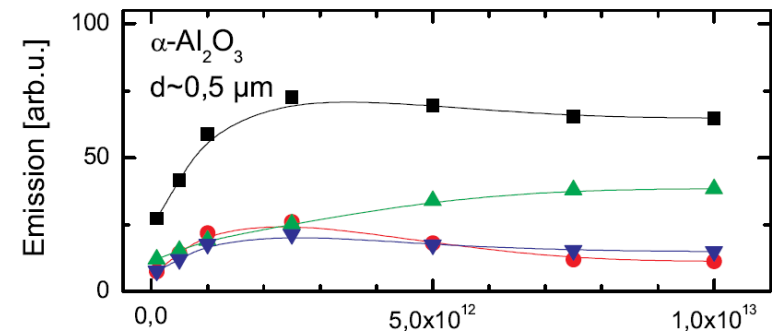
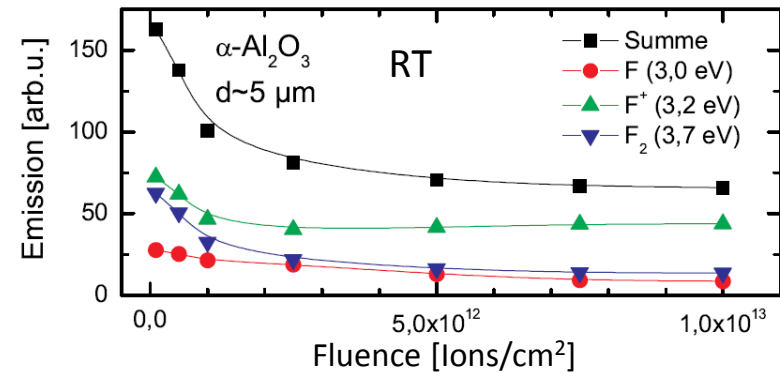
Samples from Fraunhofer Institute IKTS, Dresden

Remark:

Material modification confirmed by:

- Absorption spectroscopy
- X-ray diffraction(XRD)
- Raman scattering

⇒ F-center concentration can be determined



S. Lederer (GSI) PhD thesis

Summary and Conclusion

Investigation of Al_2O_3 as a simple intrinsic scintillator to understand relevant processes.

Experimental findings and explanation:

- **Thermal quenching** is important as it higher in the center of the beam i.e. image deformation
- For 1... 10 MeV/u ions **amorphisation** within tracks is dominant comp. to higher& lower energies
- Luminescence from color centers, **F⁺ @ 326 nm** is finally nearly constant as function of fluence
- In-situ **annealing** for $T \approx 300$ °C is possible, recovering of nearly pristine state for 700 °C for 1 h
- For high fluence nearly **equilibrium concentration** for F⁺, i.e. decrease of radiation damage
- Al_2O_3 has **large radiation tolerance** compared to other ceramics due to 'stable' F⁺ concentration

Beam diagnostics demand and possible realization:

- Scintillator measurements at **high current** LINAC with max. radiation effects and beam heating
- **Proposal:** F⁺ @ 326 nm (near UV optics, filters) with backside heater for constant F⁺ concentration
- **At GSI:** SEM-Grid is standard method for profiling: large dynamic range, no radiation damage

Pepper-pot emittance application:

- Al_2O_3 is good choice for high current and precise spot size measurement
- **But:** Due to insufficient man-power not realized at GSI, actually less interest for LINAC operation
- **Moreover:** Other problems: straggling at pepper-pot holes, dynamic range, background, noise ...
- **At GSI:** Slit-grid emittance is standard method, even though it takes up 15 min for one scan

Thank you for your attention!

Backup slides

Color Center Formation for Ceramics

Results:

- Color centers are created at all ceramics
- Different color center concentrations
- For some materials annealing by ion beam heating i.e. during irradiation

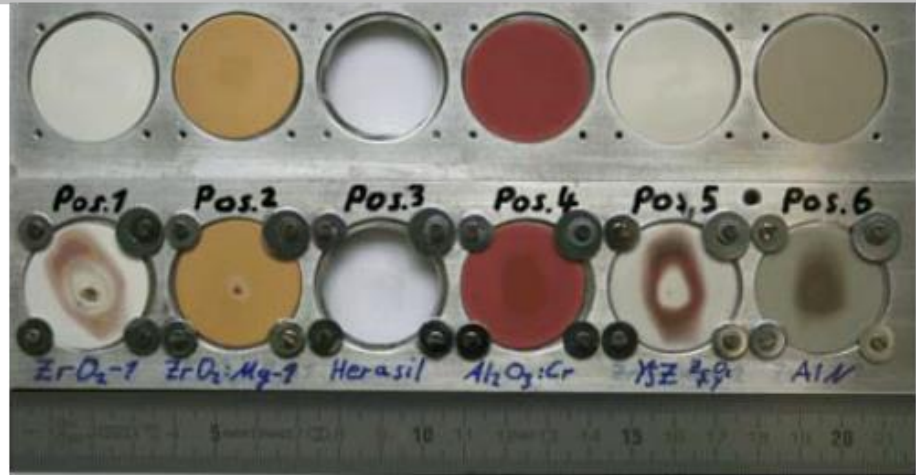
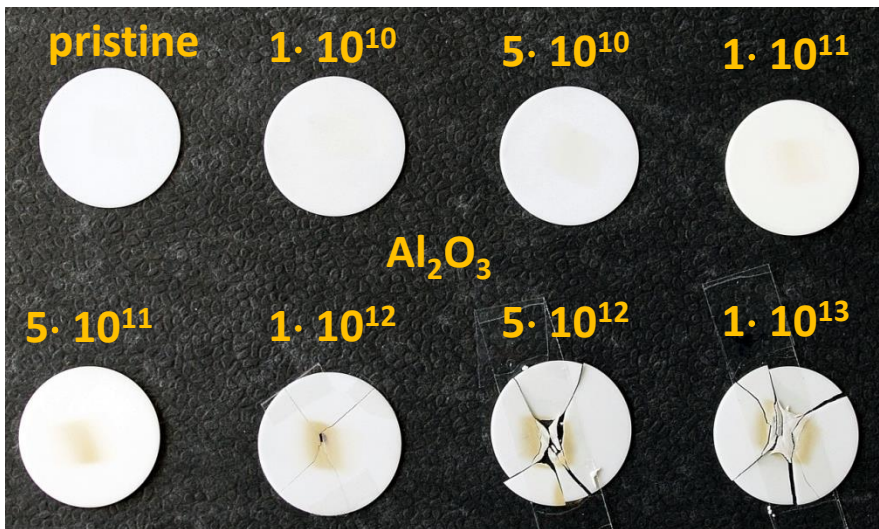
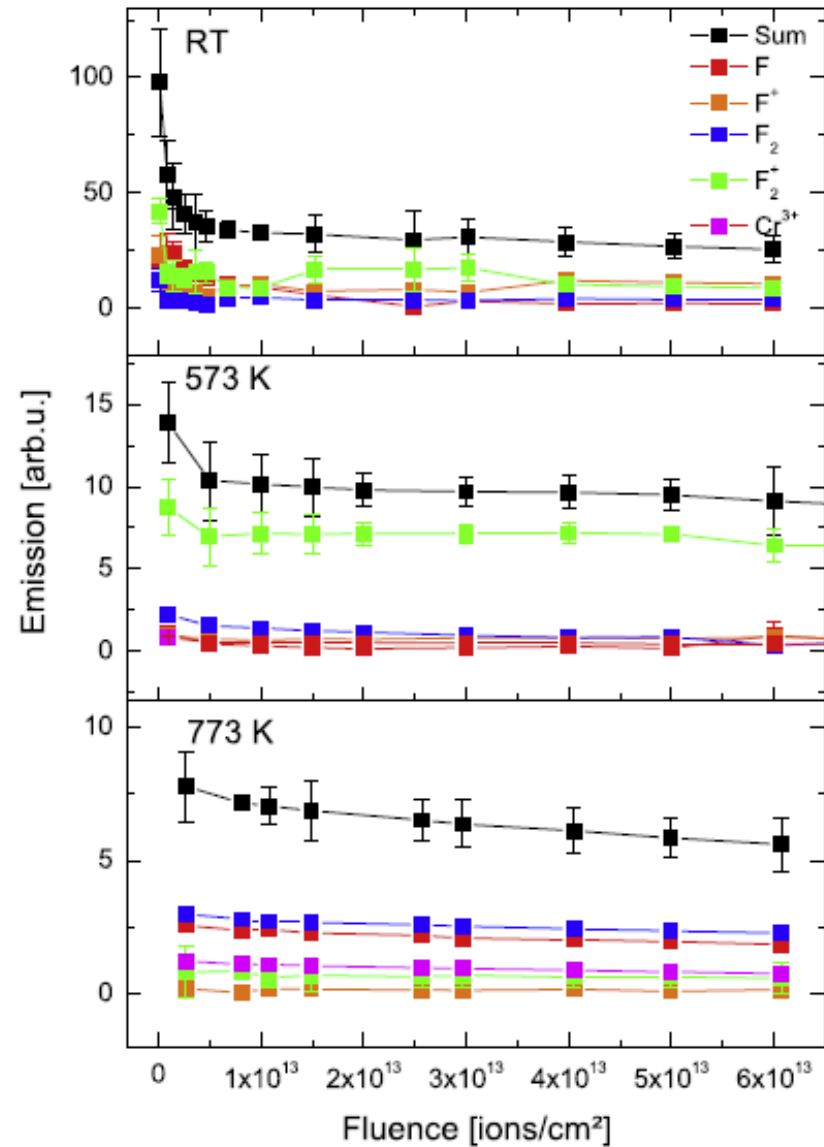


Figure 1: Target ladder with six different scintillating materials before (upper row) and after 100 pulses of U^{28+} ion beam (lower row). Beam parameters: $5.2 \cdot 10^{10}$ particles per pulse (ppp) at 4.8 MeV/u, 0.8 ms pulse length and 0.5 Hz repetition rate. Target modifications after irradiation are visible.



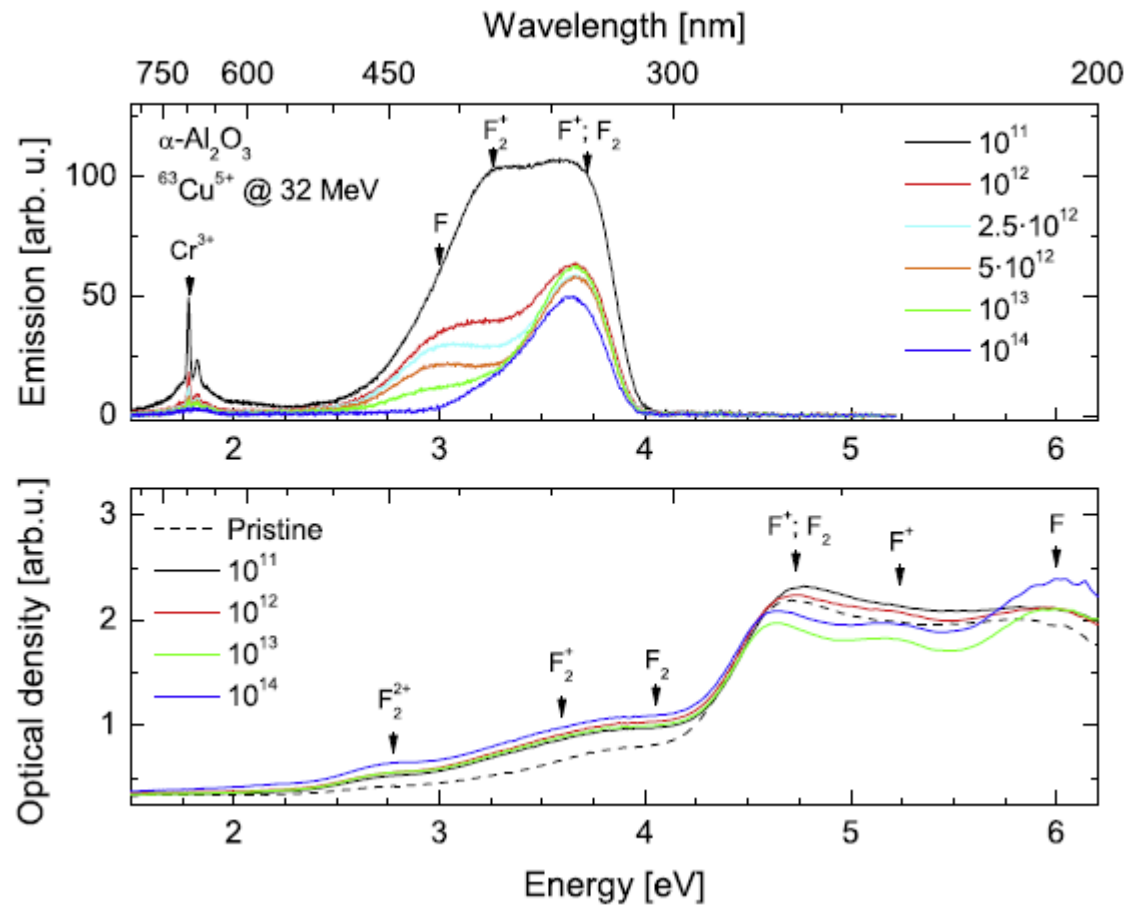
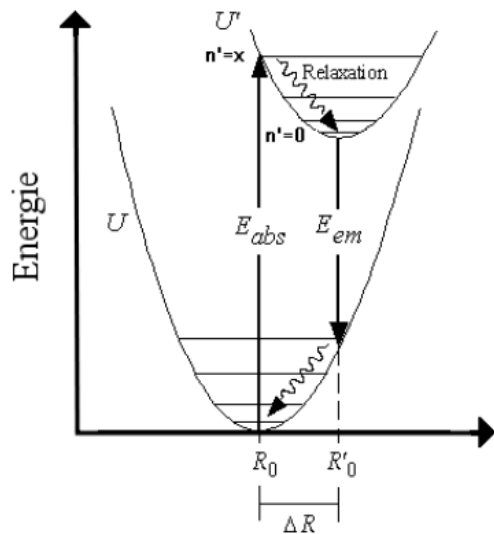
E. Gütlich (GSI) et al.



Room Temperature Emission and offline Absorption of Al_2O_3

xxx :

1. xxxx to be done
2. Partly xxx



xxx :

1. xxxx to be done
2. Partly xxx

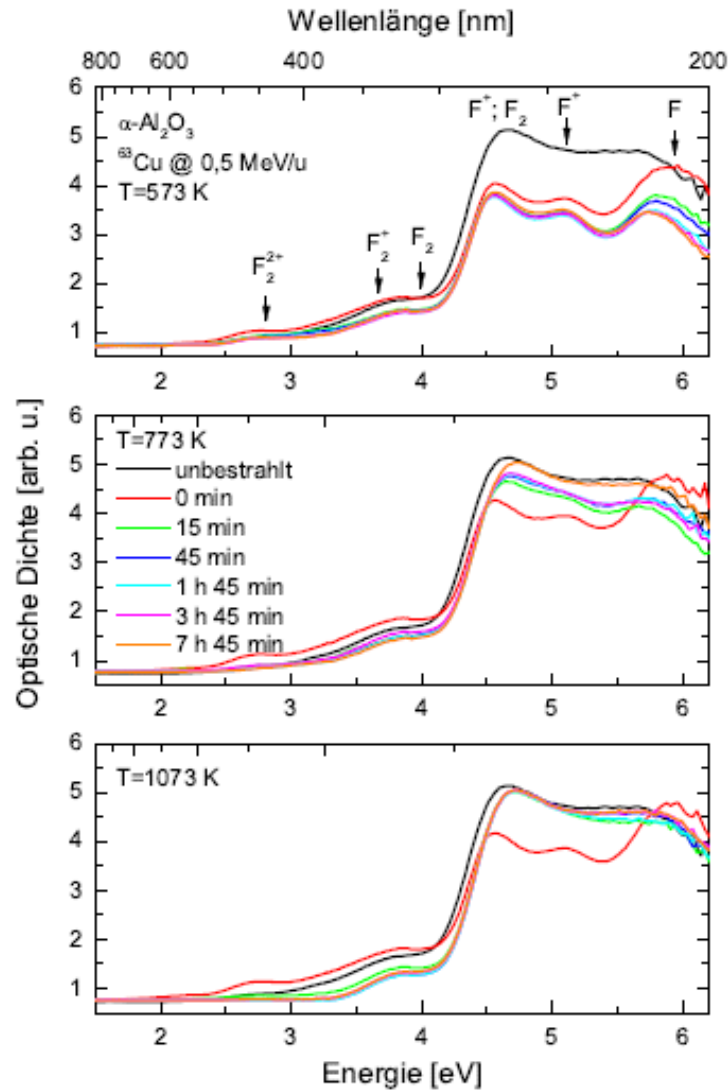


Abbildung 4.27.: Entwicklung der Absorption von $\alpha\text{-Al}_2\text{O}_3$ unter isothermen Bedingungen bei 573 K, 773 K und 1073 K.